

REPORT

 OPEN ACCESS

Extracellular-signal regulated kinase 8 of *Trypanosoma brucei* uniquely phosphorylates its proliferating cell nuclear antigen homolog and reveals exploitable properties

Ana L. Valenciano^a, Giselle M. Knudsen^b, and Zachary B. Mackey^a

^aDepartment of Biochemistry and Fralin Life Science Institute, Vector-Borne Disease Division, Virginia Polytechnic Institute and State University, Blacksburg, VA, USA; ^bDepartment of Pharmaceutical Chemistry, University of California San Francisco, San Francisco, CA, USA

ABSTRACT

The *Trypanosoma brucei* subspecies *T. brucei gambiense* and *T. brucei rhodesiense* are vector-borne pathogens that cause sleeping sickness also known as Human African Trypanosomiasis (HAT), which is fatal if left untreated. The drugs that treat HAT are ineffective and cause toxic side effects. One strategy for identifying safer and more effective HAT drugs is to therapeutically exploit essential gene targets in *T. brucei*. Genes that make up a basic mitogen-activated protein kinase (MAPK) network are present in *T. brucei*. Tb927.10.5140 encodes an essential MAPK that is homologous to the human extracellular-signal regulated kinase 8 (HsERK8) which forms a tight complex with the replication factor proliferating cell nuclear antigen (PCNA) to stabilize intracellular PCNA levels. Here we demonstrate that (TbPCNA) is uniquely phosphorylated on serine (S) and threonine (T) residues in *T. brucei* and that TbERK8 phosphorylates TbPCNA at each of these residues. The ability of an ERK8 homolog to phosphorylate a PCNA homolog is a novel biochemical property that is first demonstrated here in *T. brucei* and may be unique to this pathogen. We demonstrate that the potent HsERK8 inhibitor Ro318220, has an IC₅₀ for TbERK8 that is several hundred times higher than its reported IC₅₀ for HsERK8. This indicated that the active sites of TbERK8 and HsERK8 can be selectively inhibited, which provides a rational basis for discovering inhibitors that specifically target this essential parasite MAPK to kill the parasite.

ARTICLE HISTORY

Received 6 July 2016
Revised 3 August 2016
Accepted 4 August 2016

KEYWORDS

evolution; extracellular-signal regulated kinase (ERK); homology modeling; inhibitors; mitogen-activated protein kinase (MAPK); proliferating cell nuclear antigen (PCNA); *Trypanosoma brucei*; western blot

Introduction



Two *Trypanosoma brucei* subspecies, *T. brucei gambiense* and *T. brucei rhodesiense*, are the causative agents of Human African Trypanosomiasis (HAT) or sleeping sickness, a meningo-encephalitic disease. This parasite is endemic in the sub-Saharan region of Africa where it is transmitted by the bite of infected tsetse fly from the *Glossina* species and is most often fatal if left untreated.¹ The available HAT treatments suffer from toxic side effects, difficulty in administration, and a lack of targets that can be selectively inhibited in the parasite. The *T. brucei* genome possesses the basic components of a mitogen-activated protein kinase (MAPK) signaling network^{2,3} found in eukaryotic cells. Such networks are generally regulated by sequential phosphorylation of a 3-tiered superfamily of serine/threonine protein kinases consisting of MAPK kinase kinases, MAPK kinases, and MAPKs.^{4–6} Once activated, MAPKs phosphorylate downstream effectors that include transcription factors, protein kinases, and phosphatases.⁷ In *T. brucei*, MAPKs have been shown to regulate differentiation, stress response, and transmission in both the insect and mammalian stages of this heteroxenous parasite.^{8–11} The important role that MAPKs have in regulating many critical processes in *T. brucei* makes

them attractive for therapeutic exploitation. We previously demonstrated that depleting Tb927.10.5140 expression in bloodstream form *T. brucei* arrests proliferation and leads to its death, discovering that this MAPK is essential for the pathogenic form of the parasite.¹² We demonstrate in this study that the Tb927.10.5140 gene, which encodes an extracellular signal-regulated kinase 8 (TbERK8) homolog uniquely phosphorylates the essential replication factor proliferating cell nuclear antigen of *T. brucei* (TbPCNA) *in vitro* and in the parasite. We discuss the distinct biochemical properties of TbERK8, which opens opportunities for discovering new small molecules that can kill *T. brucei* by selectively inhibiting TbERK8.

Results

Phylogenetic analysis of TbERK8

The amino acid sequence of Tb927.10.5140 was analyzed with BLAST on the Orthologous group tool¹³ to retrieve a non-biased group of orthologous sequences. Redundant sequences were filtered out of the group while TbMAPK1 (Tb927.10.7780) and TbMAPK3 (Tb927.8.3550) were added in to optimize the ClustalW alignment among the orthologous groups. Table 1 lists the

CONTACT Zachary B. Mackey  mackeyzb@vt.edu  Department of Biochemistry, 124 Engel Hall, Virginia Polytechnic Institute and State University, Blacksburg, VA, 24061, USA.

Color versions of one or more figures in this article can be found online at www.tandfonline.com/kccy.

© 2016 Ana L. Valenciano, Giselle M. Knudsen, and Zachary B. Mackey. Published with license by Taylor & Francis
This is an Open Access article distributed under the terms of the Creative Commons Attribution-Non-Commercial License (<http://creativecommons.org/licenses/by-nc/3.0/>), which permits unrestricted non-commercial use, distribution, and reproduction in any medium, provided the original work is properly cited. The moral rights of the named author(s) have been asserted.

Table 1. ERK8 orthologs. The Tb927.10.5140 ORF was searched using BLASTO on the Orthologous group tool to retrieve an unbiased group of related eukaryotic MAPKs listed below.

| Kinase | Accession Number |
|-----------------------------|------------------|
| Tb ERK8* | Tb927.10.5140 |
| Ce ERK7 | Q11179 |
| Dm ERK7 | AAF46481 |
| Hs ERK8/MAPK15 | NP_620590 |
| Sp MAPK Spk1 | NP_594009 |
| Hs MAPK3 | NP_002737 |
| Sc MAPK1/3 fus3 | NP_009537 |
| Hs MAPK7 | NP_002740 |
| Ce MAPK-1 | CE24971 |
| Hs MAPK2 | Hs20986529 |
| Hs MAPK1 | NP_620407 |
| Hs MAPK13 | NP_002745 |
| Dm p38b | NP_477361 |
| Dm MAPK2 | NP_477163 |
| Sp Pmk1 | NP_595289 |
| Hs MAPK14 | AAP36304 |
| Hs MAPK11 | NP_002742 |
| Hs MAPK12/p38gamma | AAB40118 |
| Sc KSS1p | NP_011554 |
| Sc Kdx1p | NP_012761 |
| Hs MAPK4 | CAA42411 |
| Hs MAPK6 | NP_002739 |
| Sc Smk1p | NP_015379 |
| Ce Protein SMA-5, isoform a | NP_741909 |
| Ce NLK Isoform c | NP_001022807 |
| Ce lit-1 | NP_001022806 |
| Ce lit-1_b | NP_001022805 |
| Tb MAPK3 | Tb927.8.3550 |
| Tb MAPK1 | Tb927.10.7780 |
| SRC_tyrosine_kinase | NP_033297 |

Note. Tb: *Trypanosoma brucei*, Ce: *Caenorhabditis elegans*, Dm: *Drosophila melanogaster*, Sp: *Schizosaccharomyces pombe*, Sc: *Saccharomyces cerevisiae*, Hs: *Homo sapiens*.

genes identified from the search that were used to build this phylogenetic tree (Fig. 1A). Human sarcoma (SRC) tyrosine kinase was used as the out-group because tyrosine kinases are not encoded in the *T. brucei* genome.³ Based on the phylogenetic tree, we found that Tb927.10.5140 was located in the clade with HsERK8, whereas TbMAPK1 and TbMAPK3 were more distantly related (Fig. 1A). ClustalW alignment of Tb927.10.5140 with the open reading frame of HsERK8 demonstrated that these 2 kinases were about 36% identical at the amino acid level. The kinase domains of these 2 proteins from divergent species are about 51% identical at the amino acid level based on ClustalW alignment. Tb927.10.5140 also has a long C-terminus that extends 100 amino acids beyond the kinase domain that is not conserved, which is a defining characteristic of the ERK8 family members¹⁴ (Fig. 1B). We adopted the nomenclature of TbERK8 for Tb927.10.5140 because its coding region encodes a protein that was most closely related to HsERK8.^{12,14}

Examining the kinase activity of TbERK8

We tested TbERK8 purified from baculovirus (TbERK8_{BV}) for its ability to autophosphorylate by incubating it in buffer K that contained ³²P-γ-ATP. Autophosphorylation was determined in TbERK8 by using autoradiography to detect its incorporation of ³²P, indicating that recombinant TbERK8 purified as an active protein (Fig. 2A). We further designed a C-terminal truncated form of TbERK8 that expressed only the kinase domain residues (1-343 of TbERK8) fused to GST (GST-

TbERK8_{KD}) and re-tested its ability to autophosphorylate. The GST-TbERK8_{KD} also incorporated ³²P when incubated in kinase buffer with ³²P-γ-ATP substrate, indicating that it was able to autophosphorylate (Fig. 2B). Typically, ERKs become fully activated by upstream dual-specific MAPK-kinases that phosphorylate a conserved T-X-Y motif in the activation loop to pT-X-pY.^{7,15} ERK8 family members are atypical because full activation is catalyzed by autophosphorylation of the T-X-Y residues that make up the activation loop instead of by a dual-specific upstream MAPK-kinase.^{7,14-16} We demonstrated that TbERK8 could autophosphorylate tyrosine residues by using the PY20 antibody (Fig. 2C). The tryptic peptides of phosphorylated TbERK8 were analyzed by LC-MS/MS to further investigate if the tyrosine residue in the activation loop was phosphorylated. This analysis revealed the phosphorylated residues pT₁₇₄ and pY₁₇₆, which correspond to the activation loop motif of TbERK8 (Fig. 2D). Based on these observations, we conclude that TbERK8 has dual-specific activity that allows it to autophosphorylate the T and Y residues that make up its activation loop.

Examination of the putative TbERK8 PIP-box

Many proteins form stable interaction with PCNA through the conserved PIP-box motif. TbERK8 contains a putative PIP-box motif that is 75% identical to the functional PIP-box of HsERK8 (Fig. 1B arrows, and 3A). One of the proposed functions for the PIP-box motif of HsERK8 is to mediate its interaction with HsPCNA and form a stable complex that prevents PCNA from being degraded by the proteasome.¹⁷ We generated the GST-TbERK8-PIP-box fusion protein (GSTtbE8-PIP) depicted in Figure 3B to test the ability of this motif to interact with TbPCNA. Figure 3C shows a representative immunoblot of lysates from tetracycline-induced *T. brucei* expressing TbPCNA_{HA}. Pull-down assays were done by incubating *T. brucei* lysates from tetracycline-induced parasites with GST control (GST-Ctrl) or with GSTtbE8-PIP beads. The GSTtbE8-PIP beads pulled down about 5 times more TbPCNA than the GST-Ctrl beads (Fig. 3D and E). To assess if the putative TbERK8 PIP-box motif was fully accessible when fused to the end of GST, we did orthogonal pull down experiments using 2 canonical PIP-box motifs from unrelated proteins: (1) *T. brucei* aurora kinase 1 (TbAUK1) and (2) paraflagellar complex (TbPFC19) (Tb927.11.8220 and Tb927.10.10140, respectively). The PIP-box of either TbAUK1 or TbPFC19 was similarly fused with GST and immobilized on GST beads. We found that these 2 PIP-box motifs were respectively 5-fold and 3-fold more efficient at pulling down TbPCNA_{6H} than the TbERK8 PIP-box motif as represented by the experiments in Figure 3F. In comparison to the TbERK8 peptide sequence, the TbAUK1 and TbPFC19 PIP-boxes pulled down about 5x and 3x more TbPCNA_{6H} with *p* values of 0.045 and 0.047 respectively as determined by Student's t-test (Fig. 3G and H). This indicates that each of the motifs that we tested was exposed in our GST-fusion proteins; however, the TbERK8 motif was less efficient at pulling down TbPCNA than the TbAUK1 or TbPFC19 motifs were. We also did *in vivo* pulldown assay with hemagglutinin-tagged TbERK8 (TbERK8_{HA}) expressed in *T. brucei* followed by mass spectrometry analysis. This pull-down

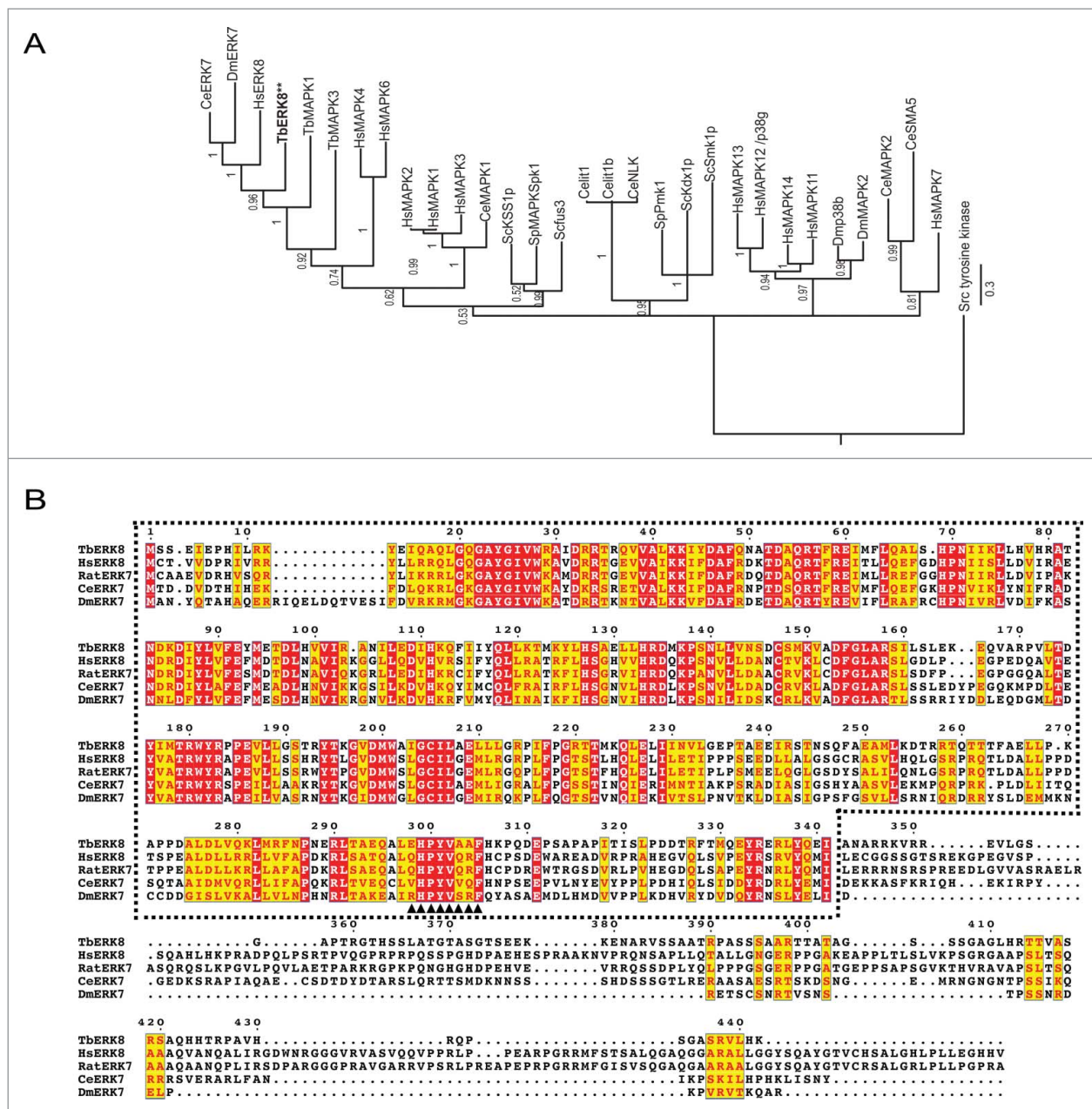


Figure 1. Phylogenetic tree and amino acid sequence alignment of ERK8-related kinases. (A) Phylogenetic relationship of the sequences and the credibility weight of the groupings were inferred using MrBayes after running 100,000 generations. Relationships with confidence values greater than 0.5 are shown at the branch points of the phylogenetic tree. The tree shown is derived from alignment with the ends trimmed to remove regions that were represented by only a few sequences. A separate analysis was done using the entire alignment and the tree topology was nearly identical to the tree shown here. (B) ClustalW alignment of ERK8 homologs. Polypeptide sequences obtained from TbERK8 BLAST on Orthologous groups were aligned using ClustalW with a gap opening penalty of 5 and a gap extension penalty of 0.05. The kinase domain is shown inside the box and the triangles (▲) highlight the PIP-box sequences. Tb: *Trypanosoma brucei*, Hs: *Homo sapiens*, Ce: *Caenorhabditis elegans*, Dm: *Drosophila melanogaster*, Sp: *Schizosaccharomyces pombe*, Sc: *Saccharomyces cerevisiae*, Rat: *Rattus rattus*.

strategy was not successful at detecting stable interactions between TbERK8 and TbPCNA (data not shown). Based on these observations, we conclude that the putative PIP-box of TbERK8 is very poor at forming a stable complex with TbPCNA in comparison with functional canonical PIP-box motifs from other *T. brucei* proteins.

Examination of TbPCNA from *in vivo* pull-down assays

The reciprocal *in vivo* pulldowns were also done with hemagglutinin-tagged TbPCNA (TbPCNA_{HA}). We immunoprecipitated

TbPCNA from stably transfected *T. brucei* strains that express wt-TbPCNA_{HA} at endogenous or overexpressed levels and subjected it to LC-MS/MS analysis. This pulldown strategy was also ineffective at detecting interactions between TbERK8 and TbPCNA (data not shown). In addition we examined the phosphorylation status of TbPCNA_{HA} pulled down from *T. brucei* by LC-MS/MS. This analysis showed that TbPCNA_{HA} pulled down from *T. brucei* was phosphorylated at residues T₂₀₂ (Fig. 4A) and S₂₁₆ (Fig. 4B) whether it was isolated from *T. brucei* that expressed it at endogenous or overexpressed levels. These phosphorylated residues are

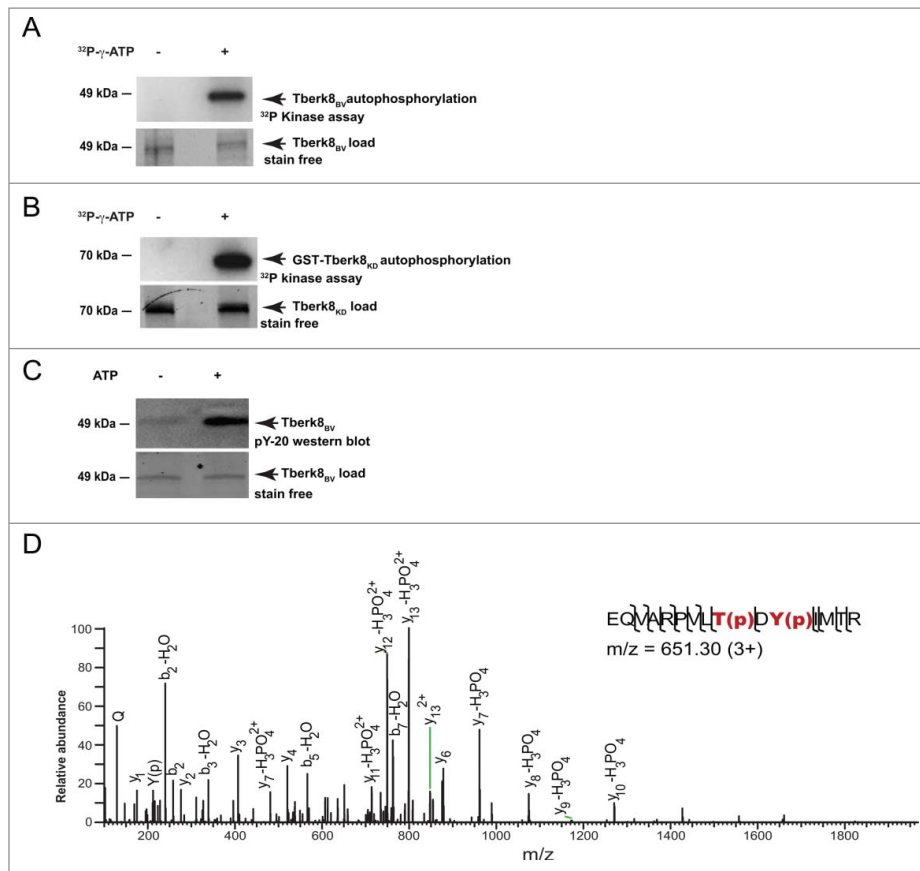


Figure 2. Autophosphorylation of TbERK8. Top panels: (A) Autoradiograph of purified recombinant TbERK8_{BV} incubated in kinase reaction buffer without (–) or with (+) 10 μ Ci 32 P- γ -ATP; (B) Autoradiograph showing the autophosphorylation of the GST-TbERK8 kinase domain (GST-TbERK8_{KD}) that lacks the C-terminus. GST-TbERK8_{KD} was tested for autophosphorylation in a kinase reaction without (–) or with (+) 10 μ Ci 32 P- γ -ATP; (C) Immunoblot using PY20 antibodies to detect phosphotyrosine residues associated with autophosphorylation of TbERK8_{BV}. Bottom panels are StainFree® gels showing the loading controls for TbERK8 samples. (D). LC-MS/MS mass spectrum of 166 EQVAREPVL(phospho)DY(phospho)IMTR₁₈₀ peptide from TbERK8 containing the phosphorylated T₁₇₄ and Y₁₇₆ residues, with $m/z = 651.30$ (3+), 0.52 ppm error.

situated in the unique insertion region of TbPCNA (Fig. 4C). Furthermore, this observation indicates that an unknown kinase activity within *T. brucei* is able to phosphorylate TbPCNA at these residues.

TbERK8 phosphorylates TbPCNA in its unique insertion

Both wt-TbERK8_{HA} and K42A-TbERK8_{HA} mutant was overexpressed in stable *T. brucei* transfectants by tetracycline induction (Fig. 5A). We demonstrated that the K42A-TbERK8_{HA} mutant was defective in 32 P- γ -ATP kinase autophosphorylation assays (Fig. S1). These overexpressed TbERK8 proteins were adsorbed to anti-HA affinity beads for use in kinase assays with buffer K and 32 P- γ -ATP to verify their activity. The generic kinase substrate myelin basic protein (MBP) and recombinant TbPCNA_{6H} purified from *E. coli* were tested as substrates in the kinase assay. The autoradiographs from the kinase assays demonstrated that TbPCNA was phosphorylated with a greater efficiency than MBP by TbERK8 immunoprecipitated from *T. brucei* (Fig. 5B). As a mock control, the affinity beads were incubated in lysates from non-transgenic *T. brucei* 221 and only background labeling of both MBP and TbPCNA was detected (Fig. 5C). When anti-HA affinity beads adsorbed with the K42A-TbERK8_{HA} mutant were used in kinase reactions, only background levels of phosphorylation similar to

those of the mock control were observed (Fig. 5D). The wt-TbERK8_{HA} phosphorylated TbPCNA_{6H} about 20-fold above the mock control and about 7-fold above the K42A-TbERK8_{HA} (Fig. 5E and F). The ability to label TbPCNA_{6H} in this kinase assay clearly depended on the K42 residue of TbERK8 being intact. We conclude from these results that the kinase activity of TbERK8 was responsible for phosphorylating TbPCNA in the kinase assay. We repeated the kinase assays with affinity beads adsorbed with wt-TbERK8_{HA} in buffer K that had cold ATP to analyze the phosphorylated TbPCNA_{6H} substrate by mass spectrometry. LC-MS/MS analysis of tryptic TbPCNA_{6H} peptides from the kinase assay identified peptides that were phosphorylated at residues T₂₀₂ and S₂₁₁ (Fig. 5G). The pT₂₀₂ residue matched the position phosphorylated in TbPCNA_{HA} immunoprecipitated from *T. brucei* and the pS₂₁₁ residues is also within the unique insertion region of TbPCNA.

We also tested TbERK8_{BV} for activity against TbPCNA using kinase buffer K with 32 P- γ -ATP. The autoradiographs from kinase reactions revealed that both TbERK8_{BV} and the 36-kDa TbPCNA_{6H} were phosphorylated (Fig. 6A). We repeated the kinase reactions in buffer containing cold ATP and resolved the phosphorylated TbPCNA by SDS-PAGE for examination by LC-MS/MS. More than 96% of the TbPCNA sequence was covered by the peptides detected by LC-MS/MS. Phosphorylated residues corresponding to S₂₁₁ (Fig. 6B) and S₂₁₆ (Fig. 6C) were identified on 2 of the peptides. The

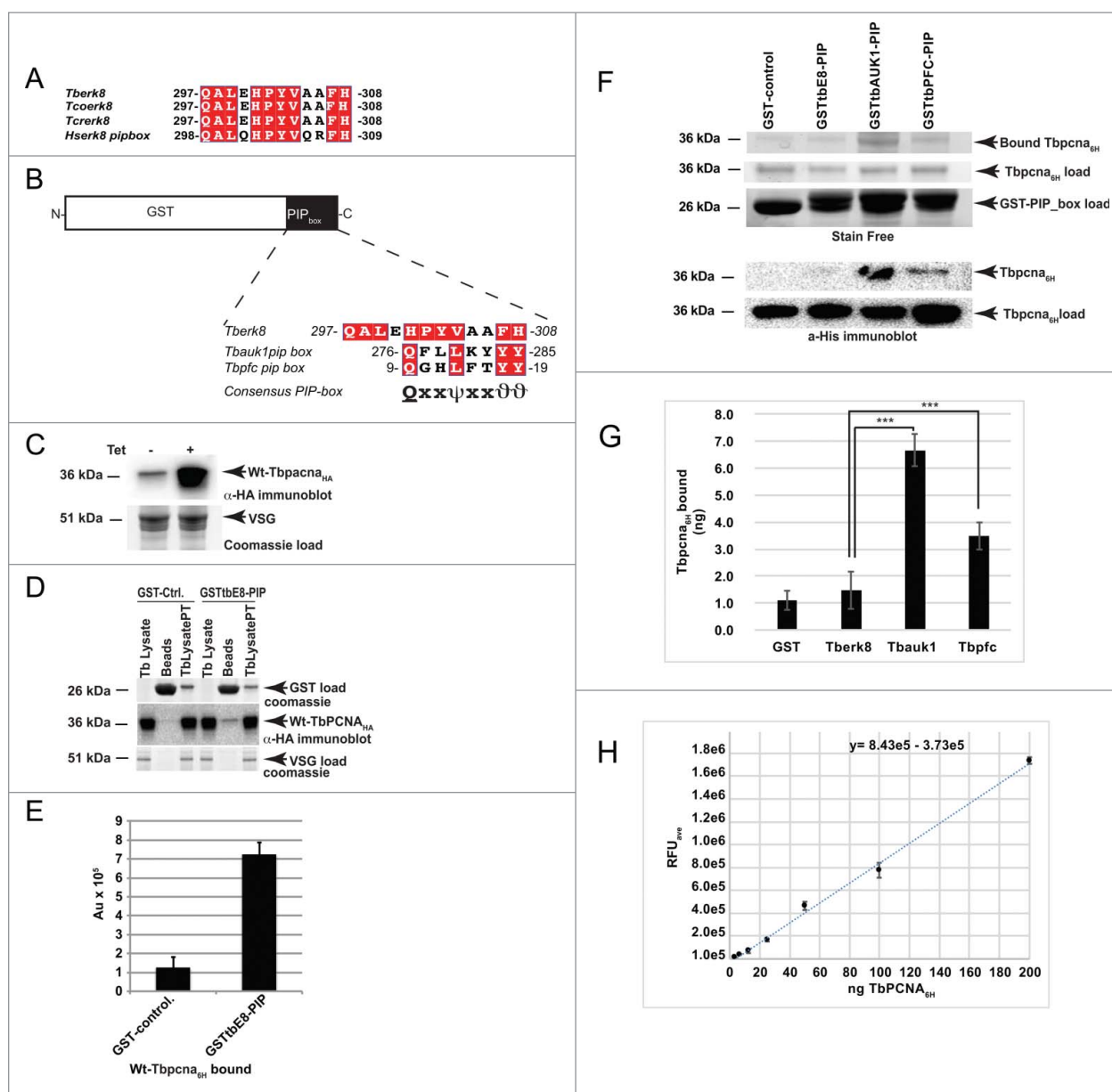


Figure 3. Testing putative TbERK8 PIP-box in TbPCNA pull-down assays. (A) Alignment of putative PIP-box motifs from ERK8 homologs of *T. brucei* (*Tb*), *T. congolense* (*Tco*), *T. cruzi* (*Tcr*), and *H. sapiens* (*Hs*). The putative PIP-box motifs are 100% identical in related trypanosome species and are 75% identical to the functional PIP-box of HsERK8. (B) Schematic presentation of GST-*T. brucei* PIP-box fusion proteins. The PIP_{box} in the schematic represents the putative TbERK8 PIP-box or canonical PIP-box sequences from TbAUK1 or TbPFC19. (C) Immunoblot analysis of wt-TbPCNA_{HA} in control (Tet -) or tetracycline-induced (Tet +) bloodstream form *T. brucei* with antisera to hemagglutinin (α-HA). Bottom panel shows Coomassie-stained gel image of variant surface antigen (VSG) loading control. (D) Examination of wt-TbPCNA_{HA} pulled down by GST-control (GST-Ctrl) or GST-TbERK8-PIP-box (GSTtbE8PIP-box) glutathione agarose beads. Top panel shows the Coomassie-stained gel image of GST fusion proteins, middle panel shows the immunoblot analysis using α-HA antibodies to detect wt-TbPCNA_{HA}, and lower panel shows Coomassie-stained gel image of VSG loading control. (E) Quantitation of wt-TbPCNA_{HA} pull down. Bar graph showing results from densitometry trace comparing the amount of TbPCNA pulled down by GST-Ctrl beads to that pulled down by GST-tbERK8-PIP beads. Values are mean arbitrary units (AU) with standard deviation for 3 independent experiments. (F) Pull down of recombinant TbPCNA_{GH} by GST-bound TbERK8 PIP-box (GSTtbE8-PIP) and GST-bound canonical PIP-boxes from TbAUK1 (GSTtbAUK1-PIP) and TbPFC19 (GSTtbPFC-PIP). The top 2 panels show StainFree® gels of TbPCNA_{GH} bound to the beads in comparison to the loading controls. The third StainFree® gels of the GST-PIP-box proteins used in pull-downs. The bottom 2 panels show the immunoblot analysis of TbPCNA_{GH} bound to the beads in comparison to the loading controls. (G) Mean quantitation values from 3 independent experiments of TbPCNA_{GH} pulled down by various GST-PIP-boxes. Error bars show standard deviation (***) indicate *p*-value < 0.05). (H) TbPCNA calibration curve from StainFree® gels showing average RFU intensity values with standard deviations from replicate experiments. (Relative Fluorescent Units, RFU), (Arbitrary Units, AU).

phosphorylated S₂₁₆ residue matched the phosphorylated serine residue identified from TbPCNA that was immunoprecipitated from *T. brucei*. The phosphorylated S₂₁₁ identified by this analysis is also located within the unique TbPCNA insertion.

In vivo phosphorylation of TbPCNA reduced upon TbERK8 depletion—We examined the effect of TbERK8 depletion on TbPCNA phosphorylation in *T. brucei* using the plasmid, pHAR (Fig. 7A). *T. brucei* stably transfected with this plasmid

simultaneously expressed HA-tagged TbPCNA under the control of the endogenous TbPCNA allele and tetracycline-inducible RNAi expression against TbERK8 mRNA. Tetracycline induction of *T. brucei* stably expressing pHAR resulted in a decrease of TbERK8 mRNA levels as well as decreased proliferation (Fig 7B). This result was consistent with our previous study of depleting TbERK8 in bloodstream form *T. brucei*.¹² We also observed that the *in vivo* levels of endogenously-tagged

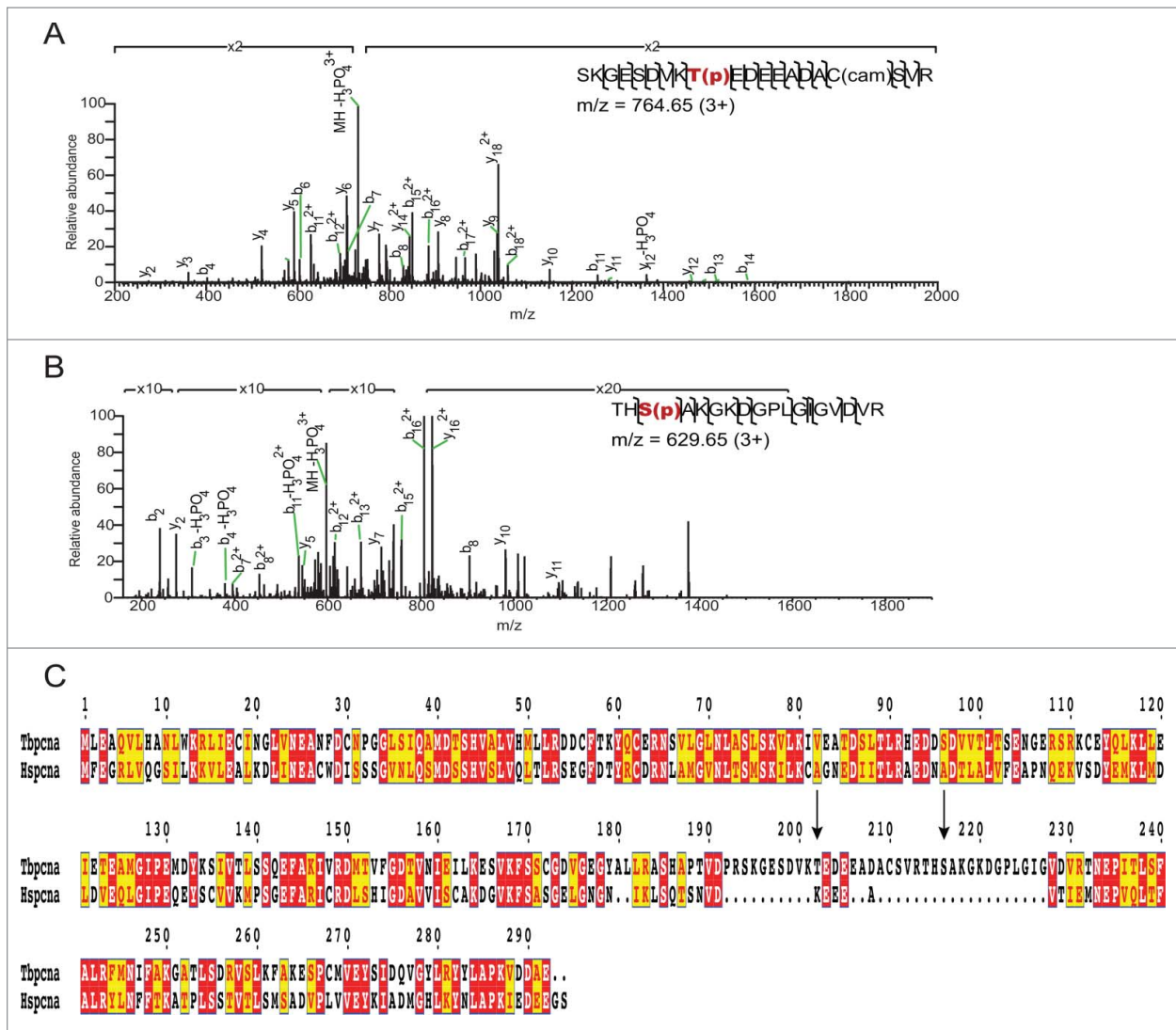


Figure 4. *In vivo* phosphorylation of TbPCNA_{HA} immunoprecipitated from *T. brucei*. (A) LC-MS/MS mass spectrum of ₁₉₄SKGESDVKT(phospho)EDEEADACSVR₂₁₃ peptide from TbPCNA containing a phosphorylated S₂₁₁ residue, with $m/z = 764.65$ (3+), 2.7 ppm error. (B) LC-MS/MS mass spectrum of ₂₁₄THS(phospho)AKGKDGPLGIGVDVR₂₃₁ peptide from TbPCNA containing a phosphorylated S₂₁₆ residue, with $m/z = 629.65$ (3+), 8.9 ppm error. (C) ClustalW alignment comparing TbPCNA with HsPCNA showing unique insertion between residues 191 and 228. Arrows show T202 and S216 residues that are phosphorylated.

TbPCNA decrease after 48 h of TbERK8 depletion (Fig. 7C). Neither T₂₀₂, S₂₁₁ nor S₂₁₆ residues were phosphorylated in TbPCNA_{HA} immunoprecipitated from *T. brucei* after 48 h of TbERK8 depletion (data not shown). The mass spectrometry analysis of the TbPCNA_{TSS} triple mutant control expressed and immunoprecipitated in *T. brucei* did not detect any phosphorylated residues. Table 2 summarizes the phosphorylated TbPCNA residues that we have identified *in vivo* and *in vitro*. We conclude that TbERK8 phosphorylates TbPCNA *in vivo*.

Small molecule inhibitors distinguish between active sites of HsERK8 and TbERK8

We probed the active site of TbERK8 with the inhibitor SCYX5070 to test for selectivity. This 2,4-diaminopyrimidine was a logical first choice because it kills *T. brucei* at submicromolar concentrations and TbERK8 (formerly annotated as Tb10.70.2070) was one of the many kinases that its immobilized version pulled down from parasite lysates.¹⁸ We tested

SCYX5070 by HTRF and determined its IC₅₀ for TbERK8 to be about 1.6 mM. At a concentration of 1 mM, SCYX5070 inhibited HsERK8 activity to 37% ± 7% versus 59% ± 11% inhibition for TbERK8 which is significantly different with a p -value = 0.02 (Fig. S2). Ro318220 is an HsERK8 inhibitor with reported IC₅₀ values that ranges from 5-10 nM.¹⁹ We tested this inhibitor at 1 μM and 10 μM against TbERK8 as shown in the representative kinase assay shown in Figure 8A. This inhibitor was able to reduce the activity of TbERK8 to 49% and 27% at 1 μM and at 10 μM respectively (Fig. 8B). Eight-point dose response curves done with Ro318220 against TbERK8 were used to calculate an IC₅₀ of 1.4 μM (Fig. 8C). This IC₅₀ of Ro318220 for TbERK8 ranges between 100 -to- 300 times higher than the IC₅₀ values of this compound reported for HsERK8.

Discussion

TbERK8 is a member of the ERK8 family of MAPKs first identified in human cells. These family members have

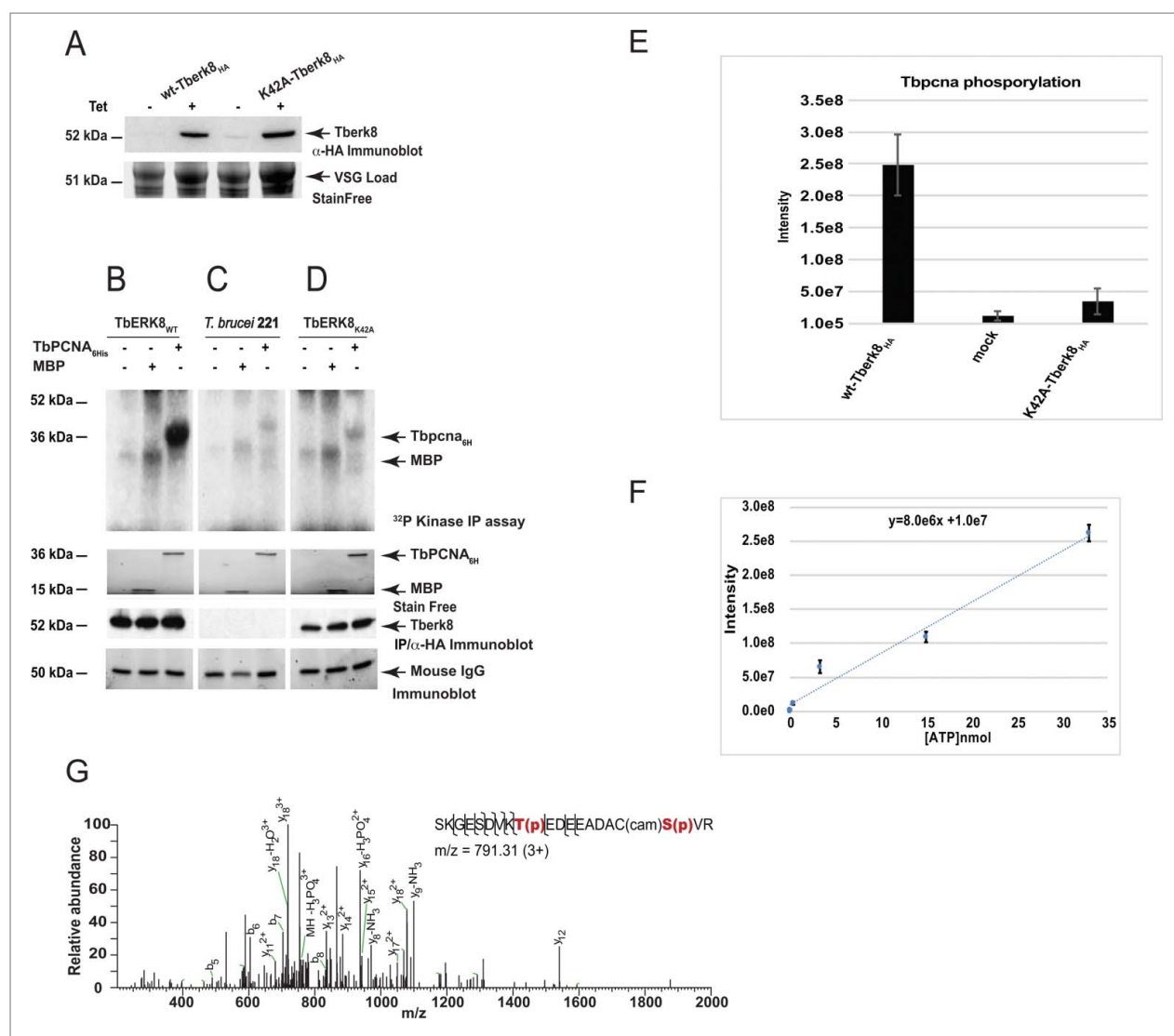


Figure 5. Activity assay with immunoprecipitated TbERK8. (A) Immunoblot verifying the expression of wt-TbERK8_{HA} and K42A-TbERK8_{HA} in the parasite after tetracycline induction (+). Arrow points to the 52-kDa HA-tagged TbERK8 band recognized by α -HA antibodies. *T. brucei* variant surface antigen (VSG arrow) was used for the loading control. ³²P-Kinase assay with wt-TbERK8_{HA} immunoprecipitated from *T. brucei*. Top panel shows the autoradiograph of kinase immunoprecipitation assays done with immuno-affinity beads pre-adsorbed with (B) wt-TbERK8_{HA}, (C) *T. brucei* 221 lysate and (D) K42A-TbERK8_{HA}. Each of the 3 sets of beads were tested with either no substrate (first lane of each experiment in the top row), 100 μ mol of MBP (second lane of each top panel), or 100 μ mol of TbPCNA (third lane of each panel). The second panel shows the StainFree[®] loading controls for MBP and TbPCNA_{6H}. The third panel shows the α -HA immunoblot detecting the HA-tagged TbERK8 bound to the immuno-affinity beads (absent in beads pre-incubated with *T. brucei* 221 lysates). The bottom panel is a α -IgG immunoblot as a loading control for the affinity beads. (E) LC-MS/MS mass spectrum of ¹⁹⁴SKGESDVKT(phospho)EED(EADAC(cam)S(phospho))VR₂₁₃ peptide from TbPCNA containing phosphorylated T₂₀₂ and S₂₁₁ residues, with m/z = 791.3165 (3+), 1.9 ppm error.

characteristically long C-terminal extensions that are not conserved.⁷ The ERK8 MAPKs are atypical because they become fully activated by autophosphorylation instead of by an upstream MAPK kinase.¹⁴ This study reveals that TbERK8 has some biochemical properties that distinguish it from its HsERK8 homolog.

We conclude that TbERK8 phosphorylates TbPCNA in *T. brucei*. By using this parasite system, we also present the first example of a PCNA homolog being phosphorylated on serine and threonine residues. All of the TbPCNA residues phosphorylated by TbERK8 identified in this study were located in an insert that is predicted to form an extended backside loop (Fig. 9A). The presence of such a loop is a feature that has only been identified in the PCNA homologs of kinetoplastid parasites. The *in vitro* kinase assays clearly demonstrated that TbERK8 was able to

phosphorylate TbPCNA_{6H} at the same residues that we identified from TbPCNA directly immunoprecipitated from *T. brucei*. Interestingly, the phosphorylation patterns of TbPCNA that was immunoprecipitated from the parasite did not exactly match those obtained from recombinant TbPCNA that was phosphorylated by recombinant TbERK8 *in vitro*. One possible explanation for such discrepancies is that an unidentified factor co-purifies with immunoprecipitated TbERK8 and regulates the way that this kinase phosphorylates TbPCNA. Our inability to phosphorylate TbPCNA with HsERK8 (Fig. S3) or to phosphorylate HsPCNA with TbERK8 (data not shown) and results from a previous study¹⁷ strengthen the hypothesis that this mechanism of PCNA serine/threonine phosphorylation is unique to *T. brucei*. However, this mechanism of PCNA phosphorylation might also be possible in other kinetoplastid parasites.

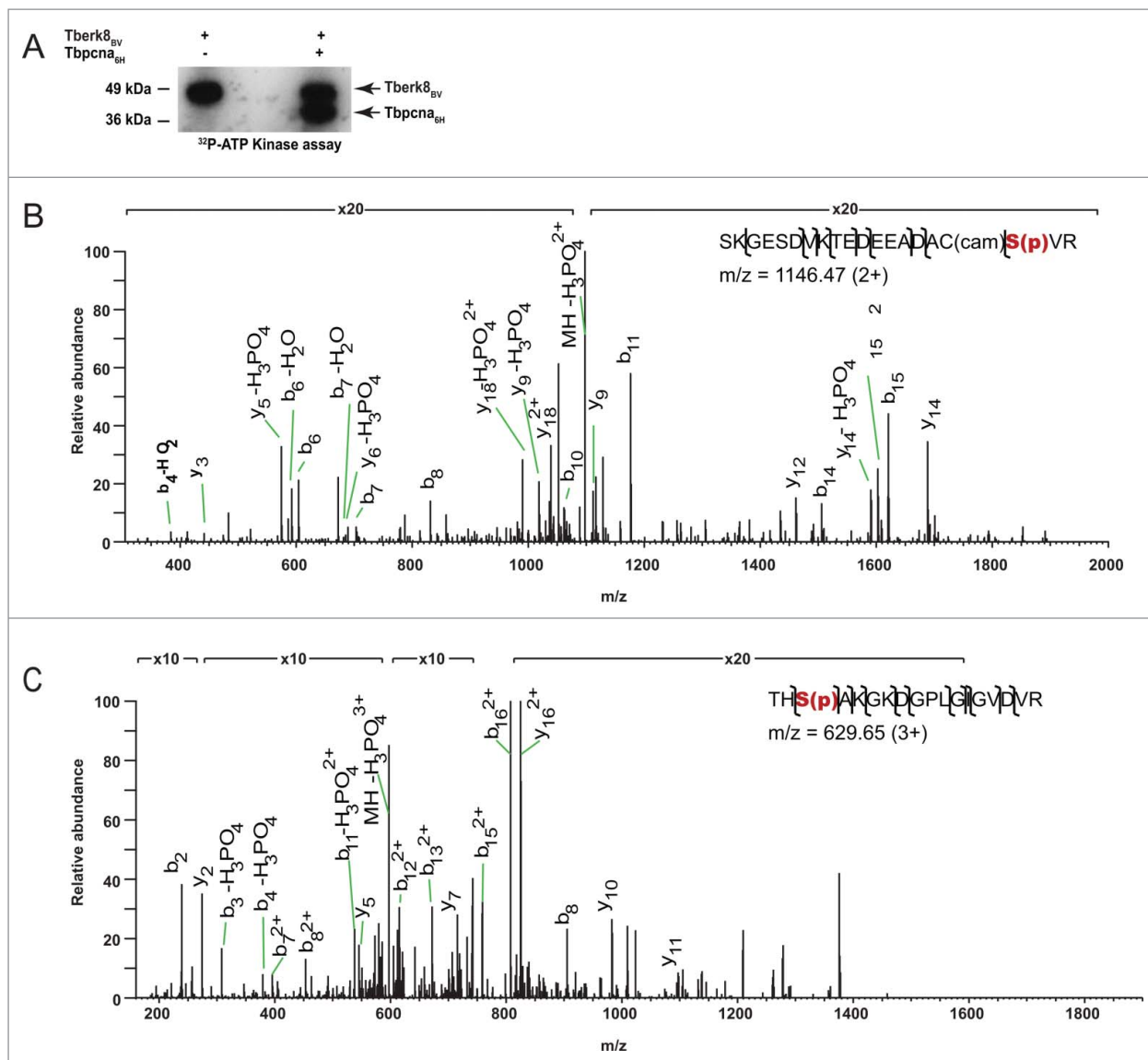


Figure 6. Recombinant TbERK8_{BV} phosphorylates TbPCNA_{BH} *in vitro*. (A) LC-MS/MS mass spectrum of ¹⁹⁴SKGESDVKTEDEEADACS(phospho)VR₂₁₃ peptide from TbPCNA containing a phosphorylated S₂₁₁ residue, with m/z = 1146.47 (2+), 5.1 ppm error. (B) LC-MS/MS mass spectrum of ²¹⁴THS(phospho)AKGKDGPLGIGVDVR₂₃₁ peptide from TbPCNA containing a phosphorylated S₂₁₆ residue, with m/z = 629.65 (2+), 1.9 ppm error.

One perceived weakness in our discovery is the observation that none of the TbPCNA residues phosphorylated by TbERK8 had a proline at the +1 position. ERKs are proline-directed serine/threonine ((S/T)P) kinases in general and such activity has been demonstrated in HsERK8.¹⁹ However, the presence of a Pro at the +1 position is not an absolute substrate requirement for ERKs and other MAPKs.^{20,21} We have identified only one potential site with a ((S/T) P) motif within TbPCNA (₂₆₃AEKSP₂₆₇), but no phosphorylated Ser₂₆₆ residue was detected by our mass spectrometry analysis of phosphorylated TbPCNA from either *in vitro* or *in vivo* preparations. We speculate that the residues that we identified by mass spectrometry represent TbPCNA sites that are the most accessible to TbERK8 and make up the majority of phosphorylation events. The other sites might represent ones that are phosphorylated at low frequencies below the detection limit of mass spectrometry analysis. The notion that TbERK8 can phosphorylate TbPCNA at other residues is strengthened by *in vitro* kinase assays using the TbPCNA_{TSS} triple mutant (Fig. S3).

All reported cases of HsPCNA phosphorylation occur on tyrosine residues.²²⁻²⁴ The phosphorylation of HsPCNA is mediated by tyrosine kinases such as epidermal growth factor receptor (EGFR)^{23,24} and the Recepteur d'Origine Nantais (RON)/c-ABL pathway.^{25,26} Receptor tyrosine kinase-mediated phosphorylation of HsPCNA occurs at Y₂₁₁ which correlates with aggressive cancer either by increased DNA synthesis activity²⁴ or inhibition of mismatch repair.²⁷ Such tyrosine kinase-mediated mechanisms of phosphorylation are not possible in *T. brucei* because the parasite lacks genes for any tyrosine kinases^{2,3} and because TbPCNA has a phenylalanine residue at the position that corresponds to Y₂₁₁ in HsPCNA (Fig. 9B).

The strengths of this study are that it reveals that the replication factor TbPCNA is the first known biological substrate for TbERK8, which is an essential MAPK in *T. brucei*. Further studies are needed to elucidate the biological role of serine/threonine phosphorylation in TbPCNA. Overall, very few substrates have been identified for ERK8 homologs. The only known cellular substrate of HsERK8 to

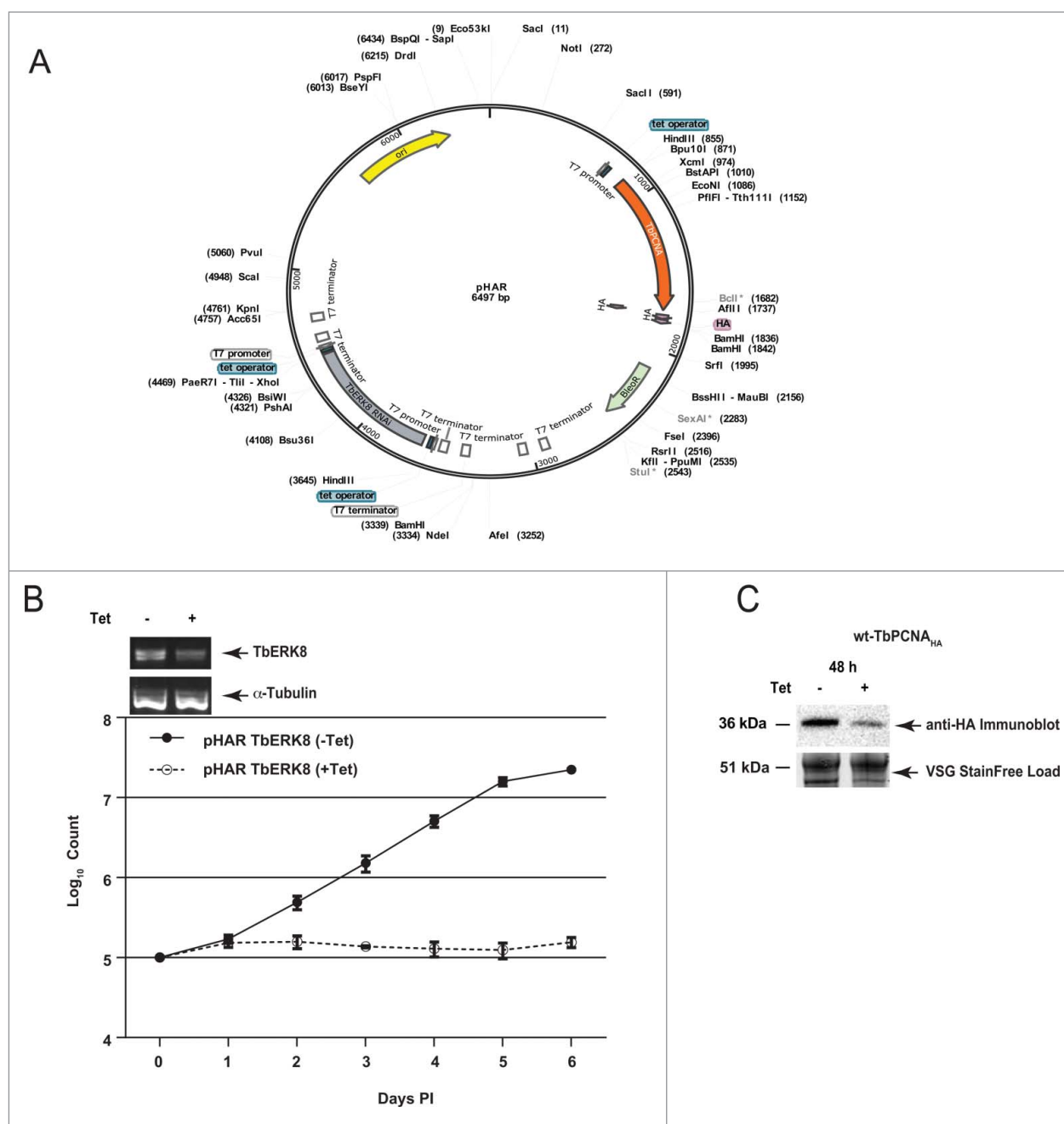


Figure 7. TbERK8 levels have an effect on TbPCNA phosphorylation *in vivo*. (A) Map of the plasmid pHAR. The plasmid has an HA-tag for endogenous expression of TbPCNA and an RNAi construct for TbERK8 silencing. (B) Decreased proliferation in pHAR stable parasites with tetracycline induction to reduce TbERK8 mRNA levels. Sybersafe gels at the top show the reduction of TbERK8 mRNA levels as detected by RT-PCR after 48 h of induction (upper panel). α -tubulin was used as a control (bottom panel). The bottom graph shows the growth curve for pHAR stable parasites with (+Tet) () or without (-Tet) () tetracycline induction for TbERK8 silencing. The growth curve represents parasite proliferation monitored during 6 d in 3 replicates. (C) Reduction in TbPCNA levels in pHAR stable parasites after tetracycline induction to reduce TbERK8 mRNA levels. Western blot shows the levels of expression of TbPCNA after 48 h of tetracycline induction (upper). The StainFree[®] gel shows VSG as a loading control (bottom).

date is the RNA binding protein HuR,²⁸ which is encoded by the *ELAVL1* gene. HuR binds to the 3'UTR of the PDC4 tumor suppressor to protect it from miRNA 21 mediated gene silencing.²⁹⁻³¹ Ro318220 is a potent inhibitor of human ERK8 and several other human protein kinases.^{19,32,33} The ability of Ro318220 to inhibit HsERK8 with such a low IC₅₀ in comparison to TbERK8 presents evidence that the active sites of HsERK8 and TbERK8 can be selectively inhibited. This creates a rational basis for discovering and developing small molecules that selectively inhibit TbERK8

to kill *T. brucei* and have fewer off-target effects in the host. TbERK8 selective inhibitors can also be used to chemically map out its biological function in *T. brucei*.

Materials and methods

Culturing of *T. brucei*

Bloodstream form parasites (Lister 427 VSG 221 strain) were incubated in 5% CO₂ at 37 °C in complete HMI-9 medium

Table 2. Summary of phosphorylated residues identified on TbPCNA immunoprecipitated from *T. brucei*.

| | pS ₂₀₂ | pS ₂₁₁ | pS ₂₁₆ |
|---------------------------|-------------------|-------------------|-------------------|
| O/E-TbPCNA _{HA} | + | – | + |
| EL-TbPCNA _{HA} | + | – | + |
| pHAR-TbPCNA _{HA} | – | – | – |

Note. Overexpressed (O/E), Endogenous Levels (EL), after TbERK8 depletion (pHAR)

purchased from Axenia Biologix (<http://www.axeniabio.com/>) using the formulation of Hirumi and Hirumi.³⁴

Primers for TbERK8 and TbPCNA constructs

The coding region for wild-type TbERK8 (wt-TbERK8) was amplified with the forward primer 5'-CGCGCCAAGCTTATGT-CAT-CAGAAATAGAGCC-3' and the reverse primer 5'-CTTAAGT-

TTGTGCAACACACGAGAGGC-3'. The K42A point mutation (K42A-TbERK8) was made in TbERK8 cDNA using the K42A forward primer 5'-GGTTGTAGCGTTAGCGAAGATATACGAC-GC3 and reverse 5'-GCGTCGTATATCTT-CGCTAACGCTA-CAACC-3' by the annealing overlapping PCR method.³⁵

The wild-type TbPCNA coding region (wt-TbPCNA) was amplified by PCR from *T. brucei* genomic DNA using the forward primer 5'-AAGCTTATGCTTGAGGCTCAG-GTTCTG-3' and the reverse primer 5'-CTTAAGCTCGGCGTCGTCCACCTT-TGG-3'. Primers to generate the PIP-box from TbERK8 were 5'-CGATACTTAAGGGATCCATGTC-CCCTATACTAGGT-3' and 5'-GCGAGA-GTCGACTCAGTGAAAGCCG-CCACATACG-G3'. Primers to generate the PIP-box from TbAUK1 were forward primer 5'-GATCCCAGTTCCTTCTCAAGTATTATTATG-3' and reverse primer 5'-TCGACATAATAATACTTGAGAAG-GAACTGG-3'. Primers to generate the PIP-box from TbPFC19 were forward primer 5'-GATCCCAGGGCCACTTGTTTA-

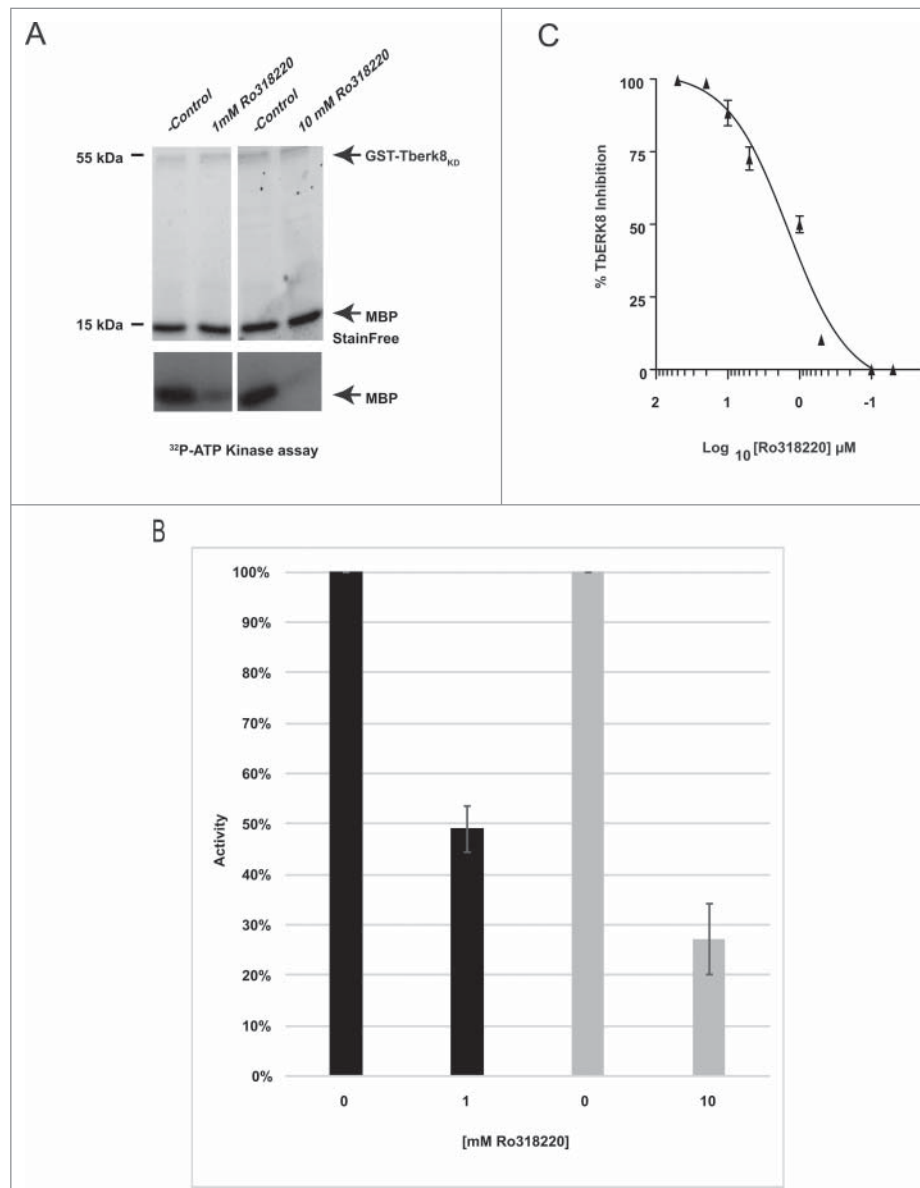


Figure 8. Testing the HsERK8 inhibitor Ro318220 against TbERK8. (A) Kinase assay using MBP as the substrate to test Ro318220 against TbERK8 at 1 μ M and 10 μ M. (B) Bar graph showing how much the activity of TbERK8 is inhibited by Ro318220 at 1 μ M and 10 μ M. (C) Eight-point dose curve of Ro318220 against TbERK8 in kinase assay using MBP to calculate IC₅₀. Graphs show the mean values and standard deviations for triplicate experiments.

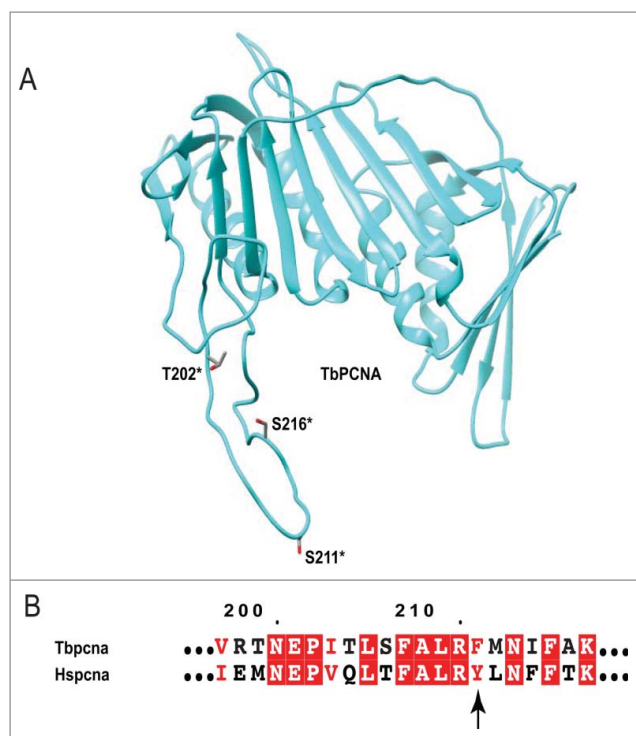


Figure 9. Model for phosphorylated TbPCNA. (A) TbPCNA model showing that the phosphorylated residues ^{*}T₂₀₂, ^{*}S₂₁₁ and ^{*}S₂₁₆ are situated in its extended backside loop formed by its unique insertions. (B) ClustalW alignment of TbPCNA and HsPCNA with black arrow showing tyrosine 211, which is phosphorylated by receptor tyrosine kinases. Note that TbPCNA has a phenylalanine residue at the corresponding position. *denotes phospho-serine/threonine residues.

CCTACTACG-3' and reverse primer 5' -TACGGTGGCCCTGG-3'. These primers were annealed and subcloned into BamHI/SalI restriction sites of pGSTag.³⁶

Expression and purification of recombinant proteins in *E. coli*

wt-TbPCNA was subcloned into the BamHI/HindIII sites of pTrcHis A (Invitrogen, <https://www.thermofisher.com/order/catalog/product/V36520?ICID=search-product>) and expressed with a 6×His tag in BL21-DE3. The recombinant protein, wt-TbPCNA_{6H}, was purified by nickel agarose affinity chromatography (Cat# 88222, Lot# PL208040, Thermo Scientific, <https://www.thermofisher.com/us/en/home.html>) as recommended by the manufacturer.

To express the TbERK8 kinase domain without the C-terminal extension, the nucleotides from 1-1019 of its coding region were subcloned into the BamHI/EcoRI sites of pGSTag to express it as a GST fusion protein (GST-TbERK8_{KD}) in *E. coli*. The full-length TbERK8 (nucleotides 1-1329) was subcloned into BamHI/HindIII site of the pGSTag to express it as a GST fusion protein (GST-TbERK8). The pGEX-2T-HsERK8 expression plasmid was kindly provided by the laboratory of Deborah Lannigan (Vanderbilt University). *E. coli* expressing either GST-TbERK8, GST-TbERK8_{KD}, or GST-HsERK8 fusion protein were grown at 37 °C until they reached an A₆₀₀ of 1.0, then chilled on ice before inducing with 0.2 mM isopropyl β-D-1-thiogalactopyranoside at 16 °C for 12 h. The *E. coli* were pelleted by centrifugation at 7,000 rpm in a Beckman JLA 10.5 rotor at 10 °C for 15 minutes. Pellets were lysed by

sonication and clarified by centrifugation at 15,000 rpm using a Beckman JA 25.5 rotor at 4 °C. These GST fusion proteins were purified by GSTPrep FF 16/10 affinity chromatography (Cat# 28-9365-50, Lot# 10233091, GE Healthcare, <http://www.gelifesciences.com/webapp/wcs/stores/servlet/ProductDisplay?categoryId=114-38&catalogId=10101&productId=17628&storeId=11787&langId=-1>) as recommended by the manufacturer.

Purification of TbERK8_{BV} from SF9 insect cells

A recombinant baculovirus encoding the full coding region of TbERK8 was constructed using the pFastBac1 baculovirus expression system (ThermoFisher Scientific, <https://www.thermofisher.com/order/catalog/product/10712024>). Sf9 insect cells (4 × 250 ml) were grown to a density of 2.0 × 10⁶ cells/ml and then infected with the recombinant virus at a multiplicity of infection of 3-5. After rotation at 150 rpm for 72 h at 28 °C, the cells were harvested by centrifugation, flash-frozen in liquid nitrogen, and stored at -80 °C. The frozen pellet was thawed on ice and then resuspended in 200 ml of 50 mM Tris-HCl (pH 7.5), 75 mM NaCl, 0.1% Nonidet P-40, 1 mM EDTA, 0.5 mM dithiothreitol (DTT), 1 mM phenylmethanesulfonyl fluoride, 1 mM benzamidine-HCl, 1 μg/ml leupeptin, 2 μg/ml aprotinin, and 1 μg/ml pepstatin. After 30 min on ice, the lysate was cleared by centrifugation at 35,000 rpm for 30 min in a Beckman 45 Ti rotor at 4 °C. The clarified lysate was loaded on a carboxymethyl (CM) chromatography column (Cat# 17-0719-01, GE Healthcare, <http://www.gelifesciences.com/webapp/wcs/stores/servlet/Home/en/GELifeSciences-us/>). Protein was eluted from the CM column with buffer A (150 mM NaCl in 20 mM Tris, pH 7.4, 10% Glycerol and 1 mM EDTA). These fractions were pooled and loaded onto hydroxyapatite (HAP) chromatography resin (Cat# 130-0151, BioRad, <http://www.bio-rad.com/en-us/category/cht-ceramic-hydroxyapatite-crySTALLINE-hydroxyapatite-resins>). TbERK8_{BV} was eluted from the HAP column in buffer B (HEPES, pH 7.4 10% glycerol, 75 mM NaCl, 75 mM phosphate ions). Fractions from the HAP column were pooled and loaded onto an S-Fast Flow column (Cat# 17-0511-01, GE Healthcare Life Sciences, <http://www.gelifesciences.com/webapp/wcs/stores/servlet/Home/en/GELifeSciences-us/>) and eluted with buffer A containing 250 mM NaCl.

Autophosphorylation of recombinant TbERK8_{BV} and GST-TbERK8_{KD}

We incubated 0.1 μg of purified TbERK8_{BV} or GST-TbERK8_{KD} protein in 30 μl of buffer K (30 mM Tris pH 7.4, 10 mM MgCl₂, 1 mM DTT, 5% glycerol, [1mM cold ATP for mass spectrometry assays or 10-100 μM cold ATP for ³²P incorporations assays] and 0.1 mg/ml bovine serum albumin). Ten μCi of ³²P-γ-ATP were added for detections by autoradiography in labeling experiments. The kinase reactions were incubated at 30 °C for 30 min. SDS loading buffer was added to the reaction mixtures and boiled for 1 min to stop the reaction. TbERK8 autophosphorylation by this method was detected by SDS-PAGE and autoradiography. Alternatively, TbERK8 autophosphorylation was done using 1 mM of cold ATP. In this case, TbERK8 autophosphorylation was detected by immunoblot analysis using the anti-phosphotyrosine antibody PY20

(Cat# GTX10321, Lot# 33072, GeneTex Inc. <http://www.genetex.com/>) at 1/500. PY20 was recognized by a horseradish peroxidase-conjugated secondary antibody to the mouse IgG2b (Cat# GTX77294, Lot# 821600258, GeneTex Inc. <http://www.genetex.com/>).

Kinase activity assays

Recombinant full-length TbERK8_{BV} purified from Sf9 insect cells (100 nmol) was incubated with 100 μ mol TbPCNA_{6H}. For activity assays, 10 μ Ci of ³²P- γ -ATP (Cat# BLU502H250UC, Perkin Elmer, <http://www.perkinelmer.com/product/atp-g-32p-blu002250uc?searchTerm=32p&pushBackUrl=?searchName=32p&No=0&Ns=Best%20Match>) were added to 30 μ L reactions that used buffer K. The samples were incubated for 5 min at 30 °C and stopped as described above. Reactions were resolved in an SDS-PAGE gel, and bands were visualized by autoradiography. TbPCNA phosphorylation was quantified with a Typhoon FLA 7000 PhosphorImager (GE Healthcare). To determine the K_m of TbERK8_{BV} for TbPCNA_{6H} kinase assays were performed with ³²P- γ -ATP and varying concentrations of purified recombinant TbPCNA_{6H} ranging from 10 nM to 5 μ M. Standard curves for autoradiography quantitation by PhosphorImager were made from 2-fold serial dilutions of 10 μ L Ci of ³²P- γ -ATP in 100 μ M cold ATP. Steady-state kinetics of TbERK8_{BV} were calculated by fitting data to the Michaelis-Menten curve using Prism Graphpad 5.0 (Fig. S4).

Expression of hemagglutinin tagged (HA-tagged) recombinant proteins in *T. brucei*

pLEW11-3HA was generated by modifying the plasmid pLEW111,³⁷ which allows for tetracycline inducible protein expression, to include a C-terminal hemagglutinin tag (HA-tag). The coding region for wt-TbERK8, K42A-TbERK8, and wt-TbPCNA were subcloned into the HindIII and AflII restriction sites of pLEW11-3HA. Nucleofections were carried out with 1 μ g to 10 μ g DNA using the Lonza Nucleofector IITM program X-001 and the NucleofectorTM kit for Human T cell transfection (Cat# VPA-1002, Lonza Pharma&Biotech, <http://www.lonza.com/products-services/bio-research/transfection.aspx>). Stable transfectants were selected based on their resistance to phleomycin. HA-tagged recombinant proteins wt-TbERK8_{HA}, K42A-TbERK8_{HA}, and wt-TbPCNA_{HA} were induced with tetracycline and expressed in the *T. brucei* 90-13 strain as described by Wirtz *et al.*³⁸ The expression of recombinant proteins was confirmed by immunodetection with rabbit anti-HA (Cat# H6908, Sigma-Aldrich, <http://www.sigmaaldrich.com/catalog/product/sigma/h6908?lang=en®ion=US>) antibody and by mass spectrometry.

pHAR construct

The TbERK8 RNAi construct from pZJM³⁹ was digested with BamHI and KpnI and subcloned into the modified pLEW11-3HA plasmid containing wt-TbPCNA. We named the resulting plasmid pHAR because of its ability to express HA tagged TbPCNA and TbERK8 RNAi cassette simultaneously. The plasmid pHAR was linearized with the restriction enzyme BsaBI, which has a unique site in the TbPCNA coding region, and 10 μ g

of the linearized plasmid was nucleofected into the Tb90-13 to produce a stably transfected *T. brucei* strain that expressed endogenous levels of HA-tagged TbPCNA and the tetracycline inducible TbERK8 RNAi cassette. TbPCNA protein levels in these parasites were monitored by immunoblot as described below.

Immunoblot analysis of HA-tagged proteins

Parasites from cultured bloodstream form *T. brucei* were harvested at 2×10^6 cells/ml, lysed with Tb lysis buffer (1.0% Triton X-100, 10 mM Tris pH 7.5, 25 mM KCl, 150 mM NaCl, 1 mM MgCl₂, 0.2 mM EDTA, 1 mM dithiothreitol, 20% glycerol), and incubated on ice for 30 min, followed by microcentrifugation at 15,000 rpm for 5 min to produce a clarified lysate. For immunoblotting, 25 μ g of clarified lysate was resolved by SDS-PAGE and transferred to a polyvinylidene difluoride membrane (PVDF). After transferring and blocking, the membrane was incubated with rabbit anti-HA (1: 2,000 dilution) for 1 h and washed 3 times for 5 min with TBST (10 mM Tris, pH 7.4, 150 mM NaCl, 0.4% Tween 20). After the third wash, horseradish peroxidase-conjugated donkey anti-rabbit IgG (1: 1,000 dilution) (Cat# 32460, Thermo-Scientific, <https://www.thermofisher.com/antibody/product/Goat-anti-Rabbit-IgG-H-L-Secondary-Antibody-Polyclonal/32460>) was added to the blots for 1 h. The blots were then washed again 3 times for 5 min each and examined by enhanced chemiluminescence (ECL) (Cat# RPN2232 GE Healthcare Life Sciences, <http://www.gelifesciences.com/webapp/wcs/stores/servlet/productById/en/GELifeSciences-us/28980926>).

TbPCNA Pull Down with GST-PIP-box Fusion Constructs—The 3 GST-PIP-box fusion proteins: TbERK8 PIP-box (GSTtbE8-PIP), TbAUK1 PIP-box (GSTtbAUK1-PIP), and TbPFC19 PIP-box (GSTtbPFC-PIP) were overexpressed in *E. coli* and captured on glutathione agarose beads (Cat# G-250-10) (Gold Bio Inc., <https://www.goldbio.com/product/1252/glutathione-agarose-resin>) following the protocol suggested by the manufacturer. Briefly, the pellets from 250 ml cultures were lysed using 10 mL of buffer 4 (50 mM Tris, 1% DOC, 0.3 M urea, pH 8, 1 mM phenylmethanesulfonyl fluoride, 1 mM benzamidine-HCL) as described by Danilevich *et al.*⁴⁰ and clarified by centrifugation (4 °C at 15,000 rpm) using a Beckman JA 25.5 rotor. GST beads (200 μ l) were added to the clarified lysate and incubated overnight at 4 °C rotating to saturate the beads. The saturated beads were washed 5 times with PBS. The washed GST agarose beads were incubated with lysates from *T. brucei* that overexpressed wt-TbPCNA_{HA} for 2 hours at 4 °C. Beads were washed 5 times with PBS, boiled in 5x SDS loading buffer, and resolved by polyacrylamide gel electrophoresis. The loading controls were visualized by Coomassie stain or by StainFree[®], (<http://www.bio-rad.com/en-us/product/mini-protean-precaster-gels/mini-protean-tgx-stain-free-precaster-gels>), which contains a trihalo compound that produces a fluorescent product when covalently crosslinked to protein tryptophan residues. These gels reduced the need to stain gels and allowed bands to be visualized with a BioRad Chem-Doc MP. TbPCNA bands were detected by immunoblots using anti-HA (Cat# MAB3834, Thermo Scientific, <http://www.emdmillipore.com/US/en/product/Anti-Polyhistidine-Tag-Anti>

body,MM_NF-MAB3834) or anti-His antibodies (Cat# H6908, Sigma-Aldrich, <http://www.sigmaaldrich.com/catalog/product/sigma/h6908?lang=en®ion=US>). Standard curves for proteins quantified with StainFree gels and ChemDoc MP were made from 2-fold serial dilutions of TbPCNA.

Immunoprecipitation of HA-tagged proteins

Stable *T. brucei* transfectants that expressed either HA-tagged TbERK8 or TbPCNA were induced with tetracycline to a final concentration of 1 $\mu\text{g}/\text{ml}$ for 24 hours. Extracts from induced parasites were pelleted by centrifugation and lysed with 1 ml of Immunoprecipitation (IP) lysis buffer on ice for 30 min (1% Triton X-100, 10 mM Tris pH 7.9, 25 mM KCl, 150 mM NaCl, 1 mM MgCl_2 , 0.2 mM EDTA, 1 mM dithiothreitol (DTT), 10% glycerol, and 1 \times complete protease inhibitor mix (Cat# 11873580001, Roche, <http://www.sigmaaldrich.com/catalog/product/roche/COEDTA-FRO?lang=en®ion=US>). Lysates were incubated with 30 μl anti-HA immuno-affinity beads from (Cat# 26181, Thermo Scientific, <https://www.thermofisher.com/order/catalog/product/26181>) and rotated overnight at 4 $^\circ\text{C}$. The beads were washed 5 times with 1 ml of IP lysis buffer.

TbPCNA_{6H} pull down with full length TbERK8_{HA}

wt-TbERK8_{HA} prepared from *T. brucei* lysates was adsorbed onto 30 μl of immuno-affinity beads and washed 5 times in 1 ml of immunoprecipitation lysis buffer. Ten microliters of the anti-HA immunoaffinity beads with wt-TbERK8_{HA} were incubated with a final concentration of 15 ng/ μl of TbPCNA_{H6} in 300 μl reactions with rotating at 4 $^\circ\text{C}$ for 2 hours. Beads were washed 5 times with 1 ml of PBS, resolved by SDS-PAGE, followed by anti-His tag immunoblotting for detection of bound TbPCNA_{6H}.

Autophosphorylation and kinase activity analysis with *in vivo* expressed TbERK8

Ten microliters of the HA-immuno-affinity beads with either wt-TbERK8_{HA} or the K42A-TbERK8_{HA} mutant bound were tested for autophosphorylation as described above. To test the activity of the *in vivo* expressed proteins, we preincubated 10 microliters of the immuno-affinity beads with 10 μM ATP, 10 μCi of ^{32}P - γ -ATP in 30 μl of buffer K. Subsequently, 100 μmol of either TbPCNA_{6H} or the generic kinase substrate myelin basic protein (MBP) (Cat# 13-110, Millipore, https://www.emdmillipore.com/US/en/product/MBP,-Dephosphorylated,MM_NF-13-110) were added, and the reactions incubated at 30 $^\circ\text{C}$ for 30 min. Reactions were stopped by adding 5 \times SDS-PAGE loading buffer and boiling for 1 minute. Ten microliters of the kinase IP reaction were resolved by SDS-PAGE and examined by autoradiography. We used a mock reaction (no substrate) for each set of experiments as well as affinity beads incubated in lysates from the non-transfected *T. brucei* 221 wild type strains as negative controls to detect background labeling.

Peptide sequencing by mass spectrometry

Peptide sequencing and protein identification was performed using liquid chromatography-tandem mass spectrometry (LC-MS/MS). For protein identification, we excised and prepared bands from SDS-PAGE gels and subjected them to in-gel trypsin digestion for peptide identification.⁴¹

Sequencing was performed using either an LTQ-Orbitrap XL or an LTQ-Orbitrap Velos mass spectrometers (Thermo Scientific, Rockford, IL), each equipped with a 10,000 psi system nanoACQUITY (Waters, City State) UPLC instrument and EZ-Spray source (Thermo Scientific). Reversed phase liquid chromatography was performed using an EZ-Spray C18 column (Thermo, ES800, Pep-Map, 3 μm bead size, 75 μm \times 15 cm). The LC was operated at 600 nL/min flow rate for loading and 300 nL/min for peptide separation over a linear gradient for 60 min from 2% to 30% acetonitrile in 0.1% formic acid. Tandem mass spectrometry experiments using the LTQ OrbitrapXL and the LTQ Orbitrap Velos instruments both used survey scans recorded over a 350-1500 m/z range. The LTQ Orbitrap XL was operated in collision induced dissociation (CID) mode, and MS/MS CID scans were performed on the 6 most intense precursor ions, with the following parameters: a minimum of 1,000 counts precursor, isolation width 2.0 amu, and 35% normalized collision energy. The LTQ Orbitrap Velos was operated in higher energy collision dissociation (HCD) mode, and MS/MS HCD scans were performed on the 6 most intense precursor ions with the following parameters: 3,000 count threshold, isolation width 2.0 amu, and 30% normalized collision energy. Internal recalibration to a polydimethylcyclsiloxane (PCM) ion with m/z = 445.120025 was used for both MS and MS/MS scans on both instruments.²²

Mass spectrometry centroid peak lists were generated using in-house software called PAVA, and data were searched using Protein Prospector software v. 5.10.17.⁴² For protein identification, searches were performed against the curated *T. brucei* 972 genome in the TriTrypDB database v 8.0 (<http://tritrypdb.org/tritrypdb/>, June, 2014) containing 30,295 entries. This database was concatenated with a fully randomized set of 30,295 entries for estimation of false discovery rate.⁴³ Data were also searched against the SwissProt database (downloaded January 11, 2012) for identification of common contaminant proteins. Peptide sequences were matched as tryptic peptides with up to 2 missed cleavages, and carbamidomethylated cysteines as a fixed modification. Variable modifications included: oxidation of methionine, N-terminal pyroglutamate from glutamine, start methionine processing, protein N-terminal acetylation, and S/T phosphorylation. Mass accuracy tolerance was set to 20 ppm for parent and 0.6 Da fragment for CID experiments, and 20 ppm for parent and 30 ppm for fragment mass error for HCD experiments.

For reporting of protein identifications from this database search, score thresholds were selected that resulted in a protein false discovery rate of less than 1%. The specific Protein Prospector parameters were: minimum protein score of 22, minimum peptide score of 15, and maximum expectation values of 0.02 for protein and 0.05 for peptide matches. Site Localization In Peptide (SLIP) scoring⁴⁴ was used to score the site assignment for phosphorylation sites, with manual validation of all reported phosphorylation spectra.

Inhibitors

SCYX5070 was a kind gift from William Janzen and Melissa A. Porter, The University of North Carolina at Chapel Hill. Ro318220 (Cat# SC-200619) was purchased from Santa Cruz Biotechnology (<http://www.scbt.com/datasheet-200619-ro-31-8220.html>). Each inhibitor was pre-incubated with 100 ng of GST-TbERK8 or GST-HsERK8 to a final concentration of 1 μ M at 30 °C for 30 minutes before performing a kinase assay using 32 P- γ -ATP. The kinase reaction was stopped by boiling in 5x SDS loading buffer then resolved by SDS-PAGE. Standard curves for autoradiography quantitation by PhosphorImager were made from 2-fold serial dilutions of 10 μ l Ci of 32 P- γ -ATP in 100 μ M cold ATP.

Disclosure of potential conflicts of interest

No potential conflicts of interest were disclosed.

Acknowledgments

We would like to thank Zhijian Jake Tu¹ in the Virginia Tech Department of Biochemistry for technical expertise with phylogenetic analyses. Janet Webster and Ling Chen in the Fralin Life Science Institute for critical reading.

Funding

This work was supported in part by Start-up fund NIFA139696, VT Drug Discovery Center VTCDD ##119286. MS analysis was performed in the Bio-Organic Biomedical Mass Spectrometry Resource at UCSF (A.L. Burlingame, Director) supported by GM103481.

Notes on contributors

AVL and ZBM performed and analyzed the experiments shown in Figures 1–8 except for mass spectrometry. GMK performed and analyzed mass spectrometry experiments shown in the manuscript. All authors reviewed the results and approved the final version of the manuscript. ZBM conceived and coordinated the study, wrote the paper, and analyzed the experiments.

References

- Jamonneau V, Ilboudo H, Kabore J, Kaba D, Koffi M, Solano P, Garcia A, Courtin D, Laveissiere C, Lingue K, et al. Untreated human infections by *Trypanosoma brucei gambiense* are not 100% fatal. *PLoS Negl Trop Dis* 2012; 6:e1691; PMID:22720107
- Berriman M, Ghedin E, Hertz-Fowler C, Blandin G, Renauld H, Bartholomeu DC, Lennard NJ, Caler E, Hamlin NE, Haas B, et al. The genome of the African trypanosome *trypanosoma brucei*. *Science* 2005; 309:416-22; PMID:16020726; <http://dx.doi.org/10.1126/science.1112642>
- El-Sayed NM, Myler PJ, Blandin G, Berriman M, Crabtree J, Aggarwal G, Caler E, Renauld H, Worthey EA, Hertz-Fowler C, et al. Comparative genomics of trypanosomatid parasitic protozoa. *Science* 2005; 309:404-9; PMID:16020724; <http://dx.doi.org/10.1126/science.1112181>
- Lewis TS, Shapiro PS, Ahn NG. Signal transduction through MAP kinase cascades. *Adv Cancer Res* 1998; 74:49-139; [http://dx.doi.org/10.1016/S0065-230X\(08\)60765-4](http://dx.doi.org/10.1016/S0065-230X(08)60765-4)
- Kolch W. Meaningful relationships: the regulation of the Ras/Raf/MEK/ERK pathway by protein interactions. *Biochem J* 2000; 351:289-305; PMID:11023813; <http://dx.doi.org/10.1042/bj3510289>
- O'Neill E, Kolch W. Conferring specificity on the ubiquitous Raf/MEK signalling pathway. *Br J Cancer* 2004; 90:283-8; PMID:14735164; <http://dx.doi.org/10.1038/sj.bjc.6601488>
- Coulombe P, Meloche S. Atypical mitogen-activated protein kinases: structure, regulation and functions. *Biochim Biophys Acta* 2007; 1773:1376-87; PMID:17161475; <http://dx.doi.org/10.1016/j.bbamcr.2006.11.001>
- Muller IB, Domenicali-Pfister D, Roditi I, Vassella E. Stage-specific requirement of a mitogen-activated protein kinase by *Trypanosoma brucei*. *Mol Biol Cell* 2002; 13:3787-99; PMID:12429824; <http://dx.doi.org/10.1091/mbc.E02-02-0093>
- Domenicali Pfister D, Burkard G, Morand S, Renggli CK, Roditi I, Vassella E. A Mitogen-activated protein kinase controls differentiation of bloodstream forms of *Trypanosoma brucei*. *Eukaryot Cell* 2006; 5:1126-35; PMID:16835456; <http://dx.doi.org/10.1128/EC.00-094-06>
- Guttinger A, Schwab C, Morand S, Roditi I, Vassella E. A mitogen-activated protein kinase of *Trypanosoma brucei* confers resistance to temperature stress. *Mol Biochem Parasitol* 2007; 153:203-6; PMID:17368580; <http://dx.doi.org/10.1016/j.molbiopara.2007.02.001>
- Morand S, Renggli CK, Roditi I, Vassella E. MAP kinase kinase 1 (MKK1) is essential for transmission of *Trypanosoma brucei* by *Glossina morsitans*. *Mol Biochem Parasitol* 2012; 186:73-6; PMID:22985893; <http://dx.doi.org/10.1016/j.molbiopara.2012.09.001>
- Mackey ZB, Koupparis K, Nishino M, McKerrow JH. High-throughput analysis of an RNAi library identifies novel kinase targets in *Trypanosoma brucei*. *Chem Biol Drug Des* 2011; 78:454-63; PMID:21668652; <http://dx.doi.org/10.1111/j.1747-0285.2011.01156.x>
- Zhou Y, Landweber LF. BLASTO: a tool for searching orthologous groups. *Nucleic Acids Res* 2007; 35:W678-82; PMID:17483516; <http://dx.doi.org/10.1093/nar/gkm278>
- Abe MK, Saelzler MP, Espinosa R, 3rd, Kahle KT, Hershenson MB, Le Beau MM, Rosner MR. ERK8, a new member of the mitogen-activated protein kinase family. *J Biol Chem* 2002; 277:16733-43; PMID:11875070; <http://dx.doi.org/10.1074/jbc.M112483200>
- Bogoyevitch MA, Court NW. Counting on mitogen-activated protein kinases—ERKs 3, 4, 5, 6, 7 and 8. *Cell Signal* 2004; 16:1345-54; PMID:15381250; <http://dx.doi.org/10.1016/j.cellsig.2004.05.004>
- Abe MK, Kahle KT, Saelzler MP, Orth K, Dixon JE, Rosner MR. ERK7 is an autoactivated member of the MAPK family. *J Biol Chem* 2001; 276:21272-9; PMID:11287416; <http://dx.doi.org/10.1074/jbc.M100026200>
- Groehler AL, Lannigan DA. A chromatin-bound kinase, ERK8, protects genomic integrity by inhibiting HDM2-mediated degradation of the DNA clamp PCNA. *J Cell Biol* 2010; 190:575-86; PMID:20733054; <http://dx.doi.org/10.1083/jcb.201002124>
- Mercer L, Bowling T, Perales J, Freeman J, Nguyen T, Bacchi C, Yarett N, Don R, Jacobs R, Nare B. 2,4-Diaminopyrimidines as potent inhibitors of *Trypanosoma brucei* and identification of molecular targets by a chemical proteomics approach. *PLoS Negl Trop Dis* 2011; 5:e956; PMID:21347454; <http://dx.doi.org/10.1371/journal.pntd.0000956>
- Klevvernic IV, Stafford MJ, Morrice N, Peggie M, Morton S, Cohen P. Characterization of the reversible phosphorylation and activation of ERK8. *Biochem J* 2006; 394:365-73; PMID:16336213; <http://dx.doi.org/10.1042/BJ20051288>
- Ashwell JD. The many paths to p38 mitogen-activated protein kinase activation in the immune system. *Nat Rev Immunol* 2006; 6:532-40; PMID:16799472; <http://dx.doi.org/10.1038/nri1865>
- Songyang Z, Lu KP, Kwon YT, Tsai LH, Filhol O, Cochet C, Brickey DA, Soderling TR, Bartleson C, Graves DJ, et al. A structural basis for substrate specificities of protein Ser/Thr kinases: primary sequence preference of casein kinases I and II, NIMA, phosphorylase kinase, calmodulin-dependent kinase II, CDK5, and Erk1. *Mol Cell Biol* 1996; 16:6486-93; PMID:8887677; <http://dx.doi.org/10.1128/MCB.16.11.6486>
- Olsen JV, Blagoev B, Gnand F, Macek B, Kumar C, Mortensen P, Mann M. Global, In Vivo, and Site-Specific Phosphorylation Dynamics in Signaling Networks. *Cell* 2006; 127:635-48; PMID:17081983; <http://dx.doi.org/10.1016/j.cell.2006.09.026>

- [23] Wang S-C. PCNA: a silent housekeeper or a potential therapeutic target? *Trends Pharmacol Sci* 2014; 35:178-86; PMID:2465521
- [24] Wang S-C, Nakajima Y, Yu Y-L, Xia W, Chen C-T, Yang C-C, McIntush EW, Li L-Y, Hawke DH, Kobayashi R, et al. Tyrosine phosphorylation controls PCNA function through protein stability. *Nat Cell Biol* 2006; 8:1359-68; PMID:17115032; <http://dx.doi.org/10.1038/ncb1501>
- [25] Zhao H, Ho P-C, Lo Y-H, Espejo A, Bedford MT, Hung M-C, Wang S-C. Interaction of proliferation cell nuclear antigen (PCNA) with c-Abl in cell proliferation and response to DNA damages in breast cancer. *PLoS One* 2012; 7:e29416; PMID:22238610; <http://dx.doi.org/10.1371/journal.pone.0029416>
- [26] Zhao H, Chen MS, Lo YH, Waltz SE, Wang J, Ho PC, Vasiliauskas J, Plattner R, Wang YL, Wang SC. The Ron receptor tyrosine kinase activates c-Abl to promote cell proliferation through tyrosine phosphorylation of PCNA in breast cancer. *Oncogene* 2014; 33:1429-37; PMID:23542172; <http://dx.doi.org/10.1038/onc.2013.84>
- [27] Ortega J, Li JY, Lee S, Tong D, Gu L, Li GM. Phosphorylation of PCNA by EGFR inhibits mismatch repair and promotes misincorporation during DNA synthesis. *Proc Natl Acad Sci U S A* 2015; 112:5667-72; PMID:25825764; <http://dx.doi.org/10.1073/pnas.1417711112>
- [28] Liwak-Muir U, Dobson CC, Naing T, Wylie Q, Chehade L, Baird SD, Chakraborty PK, Holcik M. ERK8 is a novel HuR kinase that regulates tumour suppressor PDCD4 through a miR-21 dependent mechanism. 2015.
- [29] Katsanou V, Milatos S, Yiakouvakia A, Sgantzis N, Kotsoni A, Alexiou M, Harokopos V, Aidinis V, Hemberger M, Kontoyianis DL. The RNA-binding protein Elavl1/HuR is essential for placental branching morphogenesis and embryonic development. *Mol Cell Biol* 2009; 29:2762-76; PMID:19307312; <http://dx.doi.org/10.1128/MCB.01393-08>
- [30] Lebedeva S, Jens M, Theil K, Schwanhäusser B, Selbach M, Landthaler M, Rajewsky N. Transcriptome-wide Analysis of Regulatory Interactions of the RNA-Binding Protein HuR. *Mol Cell* 2011; 43:340-52; PMID:21723171; <http://dx.doi.org/10.1016/j.molcel.2011.06.008>
- [31] Mukherjee N, Corcoran David L, Nusbaum Jeffrey D, Reid David W, Georgiev S, Hafner M, Ascano Jr M, Tuschl T, Ohler U, Keene Jack D. Integrative regulatory mapping indicates that the RNA-binding protein HuR couples Pre-mRNA processing and mRNA stability. *Mol Cell* 2011; 43:327-39; PMID:21723170; <http://dx.doi.org/10.1016/j.molcel.2011.06.007>
- [32] Bain J, Plater L, Elliott M, Shpiro N, Hastie CJ, Mclauchlan H, Klevvernic I, Arthur J, Simon C, Alessi Dario R, Cohen P. The selectivity of protein kinase inhibitors: a further update. *Biochem J* 2007; 408:297-315; PMID:17850214; <http://dx.doi.org/10.1042/BJ20070797>
- [33] Davies SP, Reddy H, Caivano M, Cohen P. Specificity and mechanism of action of some commonly used protein kinase inhibitors. *Biochem J* 2000; 351:95-105; PMID:10998351; <http://dx.doi.org/10.1042/bj3510095>
- [34] Hirumi H, Hirumi K. Continuous cultivation of *Trypanosoma brucei* blood stream forms in a medium containing a low concentration of serum protein without feeder cell layers. *J Parasitol* 1989; 75:985-9; PMID:2614608; <http://dx.doi.org/10.2307/3282883>
- [35] Bryksin AV, Matsumura I. Overlap extension PCR cloning: a simple and reliable way to create recombinant plasmids. *Biotechniques* 2010; 48:463-5; PMID:20569222; <http://dx.doi.org/10.2144/000113418>
- [36] Ron D, Dressler H. pGStag—a versatile bacterial expression plasmid for enzymatic labeling of recombinant proteins. *Biotechniques* 1992; 13:866-9; PMID:1476738
- [37] Motyka SA, Drew ME, Yildirim G, Englund PT. Overexpression of a cytochrome b5 reductase-like protein causes kinetoplast DNA loss in *Trypanosoma brucei*. *J Biol Chem* 2006; 281:18499-506; PMID:16690608; <http://dx.doi.org/10.1074/jbc.M602880200>
- [38] Wirtz E, Leal S, Ochatt C, Cross GA. A tightly regulated inducible expression system for conditional gene knock-outs and dominant-negative genetics in *Trypanosoma brucei*. *Mol Biochem Parasitol* 1999; 99:89-101; PMID:10215027; [http://dx.doi.org/10.1016/S0166-6851\(99\)00002-X](http://dx.doi.org/10.1016/S0166-6851(99)00002-X)
- [39] Wang Z, Morris JC, Drew ME, Englund PT. Inhibition of *Trypanosoma brucei* gene expression by RNA interference using an integratable vector with opposing T7 promoters. *J Biol Chem* 2000; 275:40174-9; PMID:11013266; <http://dx.doi.org/10.1074/jbc.M008405200>
- [40] Danilevich VN, Petrovskaya LE, Grishin EV. A highly efficient procedure for the extraction of soluble proteins from bacterial cells with mild chaotropic solutions. *Chem Eng Technol* 2008; 31:904-10; <http://dx.doi.org/10.1002/ceat.200800024>
- [41] Hellman U, Wernstedt C, Gonez J, Heldin CH. Improvement of an “In-Gel” digestion procedure for the micropreparation of internal protein fragments for amino acid sequencing. *Anal Biochem* 1995; 224:451-5; PMID:7710111; <http://dx.doi.org/10.1006/abio.1995.1070>
- [42] Chalkley RJ, Baker PR, Medzihradsky KF, Lynn AJ, Burlingame AL. In-depth analysis of tandem mass spectrometry data from disparate instrument types. *Mol Cell Proteomics* 2008; 7:2386-98; PMID:18653769; <http://dx.doi.org/10.1074/mcp.M800021-MCP200>
- [43] Elias JE, Gygi SP. Target-decoy search strategy for increased confidence in large-scale protein identifications by mass spectrometry. *Nat Methods* 2007; 4:207-14; PMID:17327847; <http://dx.doi.org/10.1038/nmeth1019>
- [44] Baker PR, Trinidad JC, Chalkley RJ. Modification site localization scoring integrated into a search engine. *Mol Cell Proteomics* 2011; 10:M111 008078; PMID:21490164; <http://dx.doi.org/10.1074/mcp.M111.008078>